THE JOURNAL OF HISTOCHEMISTRY AND CYTOCHEMISTRY
Vol. 20, No. 12, pp. 1006-1023, 1972

Printed in U.S.A.

STUDIES ON MICROPEROXISOMES

II. A CYTOCHEMICAL METHOD FOR LIGHT AND ELECTRON MICROSCOPY[1]

ALEX B. NOVIKOFF, PHYLLIS M. NOVIKOFF, CLEVELAND DAVIS AND NELSON QUINTANA

Department of Pathology, Albert Einstein College of Medicine, Yeshiva University, Bronx, New York 10461

Received for publication June 29, 1972

A modification of the Novikoff-Goldfischer alkaline 3,3'-diaminobenzidine medium for visualizing peroxisomes is described. It makes possible light microscopic as well as electron microscopic studies of a recently described class of peroxisomes, the microperoxisomes. Potassium cyanide (5×10^{-3} M) is included in the medium to inhibit mitochondrial staining, the pH is 9.7 and there is a high concentration of H_2O_2 (0.05%). Two cell types have been chosen to illustrate the advantages of the new procedure for demonstrating the microperoxisomes: the absorptive cells in the human jejunum and the distal tubule cells in the guinea pig kidney. Suggestive relations of microperoxisomes and lipid are described in the human jejunum. The microperoxisomes are strategically located between smooth endoplasmic reticulum that radiates toward the organelles and contains lipid droplets and "central domains" of highly specialized endoplasmic reticulum which do not show the lipid droplets. The microperoxisomes are also present at the periphery of large lipid-like drops. In the guinea pig kidney tubule there is a striking difference between the thick limb of Henle and distal tubule. The distal tubule has a population of cells with large numbers of microperoxisomes readily visible by light microscopy; these cells are not present in the thick limb of Henle. Other differences between the two are also described.

Largely from electron microscopy, Kuhn (28) in 1968 described the presence of small peroxisome-like particles in parenchymal cells in the dog perianal gland and in adenomas derived from these cells. The particles measured 0.2–0.8 μ; most possessed a "terminal plate" (27) and a few showed a noncrystalline "nucleoid." The parenchymal cells were moderately positive in the Allen-Beard staining procedure for α-hydroxy acid oxidase activity (1). Cryostat sections, postfixed in chilled acetone, were used for demonstrating the oxidase activity. Reaction product (formazan) was not localized in the particles. Rather, diffuse cytoplasmic deposits were observed.

In 1970–1971 the alkaline 3,3'-diaminobenzidine (DAB) procedure of Novikoff and Goldfischer (39) was used for electron microscopic study of nucleoid-free "peroxisome-like" organelles, generally with diameters or long axes of 0.2–0.5 μ, in cells of Henle's loop and distal convolutions of rat kidney (9), in nonciliated (Clara) cells in bronchioles and type II alveolar cells in mouse and rat lung (49) and in cells of rat adrenal cortex.[2] It is considered that the alkaline DAB methods reveal the presence of catalase (15, 19, 20, 26, 35, 38, 39).

Our attention was drawn to guinea pig small intestine by the report of Connock and Pover (10) that homogenates contained catalase-rich particles, presumably peroxisomes. However, we were unable to see peroxisomes by light microscopy when sections were incubated in the optimal alkaline DAB procedure for catalase (39). This led us to modify the procedure, as described below.

The major innovation was the addition of KCN to the medium in order to remove the background staining of mitochondria; this action of KCN had been noted earlier (38, 39). For light microscopy such mitochondrial staining is troublesome because microperoxisomes may be very small and may require long periods of incubation. Thus, they become obscured by the background staining of mitochondria

[1] This work was supported by U.S. Public Health Service Research Grant R01CA06576 to Dr. A. B. Novikoff. Dr. Novikoff is the recipient of U.S. Public Health Service Research Career Award 5K6CA14923 from the National Cancer Institute.

even at alkaline pH where mitochondrial staining is markedly suboptimal (4, 5, 35, 39). This is especially true of the two cell types illustrated here, absorptive cells of the human small intestinal mucosa and epithelial cells of the distal tubules of the guinea pig kidney, and in other cell types where the microperoxisomes are clustered in the same regions in which mitochondria are concentrated.

With the new medium it is feasible to survey tissues for microperoxisomes by light microscopy of frozen sections. This medium has made possible the light microscopic study of these organelles in human liver, in which previous cytochemical methods have generally proved inadequate for visualizing peroxisomes. The studies on human liver will be described in the following publication of this series (47).

By the improved DAB procedure we were able, in the first publication of this series (46), to demonstrate huge numbers of microperoxisomes in absorptive cells of guinea pig and rat small intestine. The presence of multiple continuities with smooth endoplasmic reticulum (ER) and an irregularly granular content lacking nucleoids led us to consider these peroxisomes sufficiently different from the larger peroxisomes of hepatocytes and cells of the proximal convoluted renal tubules to warrant a new name. We wrote, "Although the distinctive relationship of these peroxisomes to the ER is probably more significant than their small size, for practical purposes we propose the term 'microperoxisomes' to distinguish these peroxisomes from the better-known larger peroxisomes of liver and kidney" (46).

In the fifth publication in this series (41) we describe a wide variety of cell types that we have studied. All possess microperoxisomes but their number varies greatly, suggesting that their functional importance differs in different cell types.[3]

[2] Beard ME: Unpublished data. This and work from other laboratories on the adrenal gland has appeared recently (3, 6, 31).

[3] A report by Hruban *et al.* (Lab Invest 27:184, 1972), which appeared when publication was in galley form, has extended further the number of cell types in which these small organelles have been reported. The authors continue to use the morphologic term, microbody, for such organelles despite the absence of nucleoids—the morphologic hallmark of hepatic and renal microbodies. Hruban *et al.* report that the "close spatial relationship ... to ... smooth endoplasmic reticulum was observed less frequently than occurs in hepatocytes." However, it is highly probable that higher magnifications of more adequately preserved material, particularly if viewed in tilted specimens (46), would reveal numerous slender continuities with smooth ER, an essential feature of microperoxisomes.

MATERIALS AND METHODS

The effects of varying the constituents of the alkaline DAB medium (39), hereafter to be called the pH 9.0 medium, were studied with guinea pig duodenum, jejunum, ileum and kidney, fixed in cold glutaraldehyde (56) or glutaraldehyde-paraformaldehyde mixtures (32, 61) for 30 min to 4 hr and in paraformaldehyde for 4 hr and overnight, as detailed earlier (46). Electron microscopy was used whenever required but light microscopy sufficed for most observations.

The medium was buffered with 0.05 *M* propanediol and the pH was varied, in steps of 0.5, from pH 8.0 to 11.0. Three concentrations of DAB-tetrahydrochloride (Sigma Chemical Company) were tried: 10, 20 and 40 mg/10 ml of medium. The final concentration of H_2O_2 was varied from 0.001 to 0.3% in closely graded steps and also 0.5, 1 and 2%. The H_2O_2 requirement was tested by omitting it from the medium, with and without the addition of catalase (1 mg/ml of medium) (15). The final concentrations of KCN tested varied from 5×10^{-6} to 1×10^{-2} *M*. The effects of heating sections for 10 min in water at 95°C were also studied.

Incubations were conducted at 37°C. Incubation times varied considerably from one tissue to another. Thus, for light microscopy 10 min of incubation in the optimal pH 9.7 medium sufficed for strong staining of microperoxisomes (and peroxisomes) in rat hepatocytes (47), 20–30 min for the microperoxisomes in the distal tubule cells of guinea pig kidney and 90–180 min in small intestine epithelium. When prolonged incubation was used, the medium was replaced by newly prepared medium every 60 min. For electron microscopy shorter incubation times were generally employed.

Sectioning and other steps in processing tissues for light microscopy or electron microscopy were the same as those described earlier (46).

A portion of jejunum was removed from a 72-year male patient at the time of left hemicolectomy for carcinoma of the splenic flexure, because of fibrous adhesions to the colon. For 4 days prior to surgery the patient had been maintained on a liquid diet high in fat and protein. Food by mouth was then withheld for 12 hr. During the 4 days preceding surgery he also had 3 tbsp mineral oil daily.

Grossly, the jejunum was normal. Checks upon its morphologic normality included histologic and cyto-

chemical preparations, as follows: *histology*, paraffin sections stained by hematoxylin-eosin, periodic acid-Schiff and Masson's trichrome procedure; *cytochemistry*, 10-μ frozen sections of appropriately fixed tissue incubated for enzyme activities which reveal different cytoplasmic organelles, by procedures used in our laboratory as markers for the different cytoplasmic organelles (33, 40).

For study of the cells in the distal convolutions, kidneys of male and female albino guinea pigs, weighing 350–700 g, were used. One kidney was removed from an etherized guinea pig, quickly cut to include cortex and medulla and placed into fixatives. Thin slices of specific areas were then made and put in fresh fixatives. Frozen sections were stained by the DAB procedures and the other cytochemical procedures were used as markers for cytoplasmic organelles (33, 40). In addition, the pararosaniline procedures of Davis and Ornstein (11) were used, with naphthol AS-TR phosphate (Sigma) for acid phosphatase (2), naphthol AS-BI glucuronide (Sigma) for β-glucuronidase (23, 24) and naphthol AS-LC N-acetyl-β-D-glucosamine (Sigma) for β-glucosaminidase (22, 23). In addition, serial 1.5-μ sections were prepared of Epon-embedded tissue incubated in DAB at pH 9.7. Twenty-seven consecutive sections were studied with oil immersion.

RESULTS

Optimal DAB medium: There is no noticeable effect of the various fixatives upon the DAB reactivity of microperoxisomes. The 30-min fixations often give weaker reactions, suggesting that better preservation of structural integrity is required for retaining all catalase (and/or oxidized DAB) within the microperoxisomes.

When the DAB-tetrahydrochloride is increased from 10 to 20 mg/10 ml, staining is somewhat stronger. Increasing the amount to 40 mg has no effect.

From pH 8.0 to 9.5 there is a steady increase in the intensity of microperoxisome staining. Between 9.5 and 11.0 the staining intensity remains the same.[4]

The higher the H_2O_2 concentration the more intensely do the microperoxisomes stain until a final concentration of 0.05% is reached. At 0.3% and higher concentrations an over-all brown color develops in which the microperoxisomes are not visible.

Potassium cyanide inhibits mitochondrial staining at a concentration of 1×10^{-3} *M*, but it has no effect upon microperoxisome staining at the highest concentration tried, 1×10^{-2} *M*.

On the basis of these observations a medium was chosen for optimal staining of microperoxisomes. This is shown in Table I, expressed both as the ingredients added and as final molarities. The medium is adjusted to pH 9.7 before addition of the H_2O_2 and it is filtered shortly after H_2O_2 addition. This medium is also optimal for the larger peroxisomes in mammalian hepatocytes and in the proximal tubules of mammalian kidney.

An absolute requirement for H_2O_2 for microperoxisome staining is indicated by abolition of their staining in the distal convolution of guinea pig kidney when catalase is added to the medium in which no exogenous H_2O_2 is present. The same is true of the peroxisomes in the proximal convolutions and, as shown by Fahimi (15), in rat hepatocytes. Complete inhibition of staining is obtained by simply omitting H_2O_2 from the medium, if the incubation time is not prolonged. At 120 min of incubation an extremely small population of proximal convolution peroxisomes are slightly positive by light microscopy, but the distal convolution microperoxisomes are negative, except for very few in occasional cells. At 160 min of incubation microperoxisomes stain lightly, apparently in all cells which would show stained organelles with H_2O_2 in the medium. However, with catalase in the medium all structures are negative, including erythrocytes. Erythrocytes are the only structures which stain in heated sections (10 min, 95°C water); such staining is lost entirely if H_2O_2 is omitted from the medium.

The advantages of the new procedure for demonstrating microperoxisomes are seen in Figures 1–4.

Absorptive cells in human jejunum: The normality of the specimen, judged in the gross, is confirmed by all histologic and cytochemical procedures used. The cytochemically demonstrable enzyme activities and distributions of organelles visualized by these activities are the same as those observed in our laboratory in rat jejunum (see Fig. 5 in Reference 34), except that alkaline phosphatase activity is not evident in the Golgi apparatus.

The absorptive cells in human jejunum, like those of guinea pig jejunum, duodenum and ileum and rat duodenum (46) and small intestine of other mammals (41), have enormous numbers of microperoxisomes. They are not evident in the *light microscope*

[4] It should be noted that 5×10^{-3} *M* $MnCl_2$ is effective in stimulating the staining of microperoxisomes, strikingly so in some cell types. However, it cannot be used at pH's above 8.5 since it precipitates as the hydroxide. Similarly if 5×10^{-3} *M* KCN is used to inhibit mitochondrial staining at pH 8.0, concentrations of H_2O_2 even as high as 0.02% which are used in the pH 8.0, high H_2O_2 medium (35, 37) result in heavy precipitates. However, in the pH 8.0, low H_2O_2 medium (35, 37), in which the final H_2O_2 concentration is 0.001% and which contains 5×10^{-3} *M* $MnCl_2$, microperoxisomes stain. In some cell types, such staining approaches that in the pH 9.7 medium.

TABLE I

Optimal DAB Medium for Microperoxisome Staining

Ingredients (per 10 ml)	Final Concentration
DAB-tetrahydrochloride,[a]	*M*
20 mg	5.6×10^{-3}
Propanediol buffer, 0.05 *M*, pH 9.0, 9.3 ml	4.65×10^{-2}
Adjust pH to 9.7 with NaOH	
KCN, 0.1 *M*, 0.5 ml	5×10^{-3}
H_2O_2, 2.5% (freshly prepared from 30% H_2O_2),[b] 0.2 ml	1.47×10^{-2} (0.05%)

[a] Sigma.

[b] Merck and Company.

with the pH 9.0 medium (Fig. 1) but are readily seen with the pH 9.7 medium. The photograph (Fig. 2) shows many fewer microperoxisomes than can be seen by focusing at the microscope.

Electron microscopy reveals that most microperoxisomes are arranged in clusters (Figs. 5, 6, 10 and 11). Examination of a cluster shows the microperoxisomes to be situated at transitional areas in the organization of smooth ER. Most of the smooth ER in these absorptive cells appears to meander gently, apparently randomly, with anastomoses at frequent intervals. The ER acquires a roughly radial arrangement as it approaches the microperoxisomes (Figs. 6, 7 and 10–12). It then continues into a "central domain" consisting of specialized ER. Within the domain the smooth ER displays its highest degree of structural order (Figs. 5, 6, 11 and 12). There are numerous anastomoses among tubules that are more compact (sometimes almost linear) and narrower than either the radiating or random smooth ER. Within the domains both membrane and cisterna appear more electron-opaque than in the ER elsewhere. To a lesser degree the cytosol outside the ER tubules also shows a somewhat greater electron opacity than the cytosol elsewhere.

The microperoxisomes are situated at the periphery of the central domains. As many as seven or eight microperoxisomes may be seen surrounding the central domain in Figure 6. It is likely that many more microperoxisomes surround the central domain in planes other than that of this random thin section. The microperoxisomes show many continuities with the smooth ER at the transition between radial ER and central domain.

Droplets with the morphologic appearance of lipid (8) are seen within the smooth ER that radiates toward the microperoxisomes and in the ER peripheral to the radiating channels (Figs. 6, 7, 10 and 12). None is seen in the ER of the central domains.

Occasionally, mitochondria are seen closely apposed to the central domains (Fig. 12).

As in guinea pig and rat intestine, the microperoxisomes appear as dilations of smooth ER with membranes of the two continuous in many places (small arrowheads, Figs. 6–12). Rough ER is almost never encountered in the regions of microperoxisomes. Perhaps because of deposition of oxidized DAB, the inner content of the microperoxisomes appears as irregular strands often radiating out toward the delimiting membrane of the microperoxisome (Figs. 6–12). The radiating strands are more evident than in guinea pig or rat (Figs. 23, 24 and 35 in Reference 46). Most (92%) microperoxisomes range from 0.13 to 0.30 μ in diameter, averaging 0.20 μ; 8% are larger, extending to 0.50 μ.

Commonly encountered are relatively large circular areas of amorphous lipid-like material. These presumably spherical bodies are marked by X's in Figures 5, 11 and 12. They lie in or near the Golgi zone. They are surrounded by small vesicles (transverse sections of tubules?) and tubules. Some of the tubules connect to smooth ER (arrows, Fig. 11). Apparent vesicles of varying size lie in the Golgi zone. There is a resemblance of some of these to the structures seen at the periphery of the spherical bodies (Figs. 11 and 12). Microperoxisomes are seen at the periphery of the lipid-like spheres (Figs. 5, 11 and 12). ER tubules apparently continuous with these spheres are also in continuity with the microperoxisomes (Fig. 11).

Figure 9 shows a microperoxisome within an apparently early autophagic vacuole. It is still DAB-reactive and continuity between the membrane of microperoxisome and ER remains (arrowhead). Only one other autophagic vacuole was encountered; this showed ER but no microperoxisome within it.

Cells in distal convolutions of guinea pig kidney: By *light microscopy*, with the new alkaline DAB procedure (Fig. 4) but not with the pH 9.0 procedure (Fig. 3) the distal convolutions show two types of cells, one with enormous numbers of dotlike DAB-positive microperoxisomes and the other without visible microperoxisomes (also without the larger peroxisomes such as seen in cells of the proximal convolution (Figs. 3 and 4)). The DAB-negative cells remain negative even after 210 min of incubation. The difference between DAB-positive and DAB-negative cells is not due to geometric differences in relation to the plane of sectioning. Oil immersion examination of serial 1.5-μ sections through entire cells shows the DAB-negative cells to be negative throughout.

The distal convolutions also show cell heterogeneity in the other cytochemical tests employed.

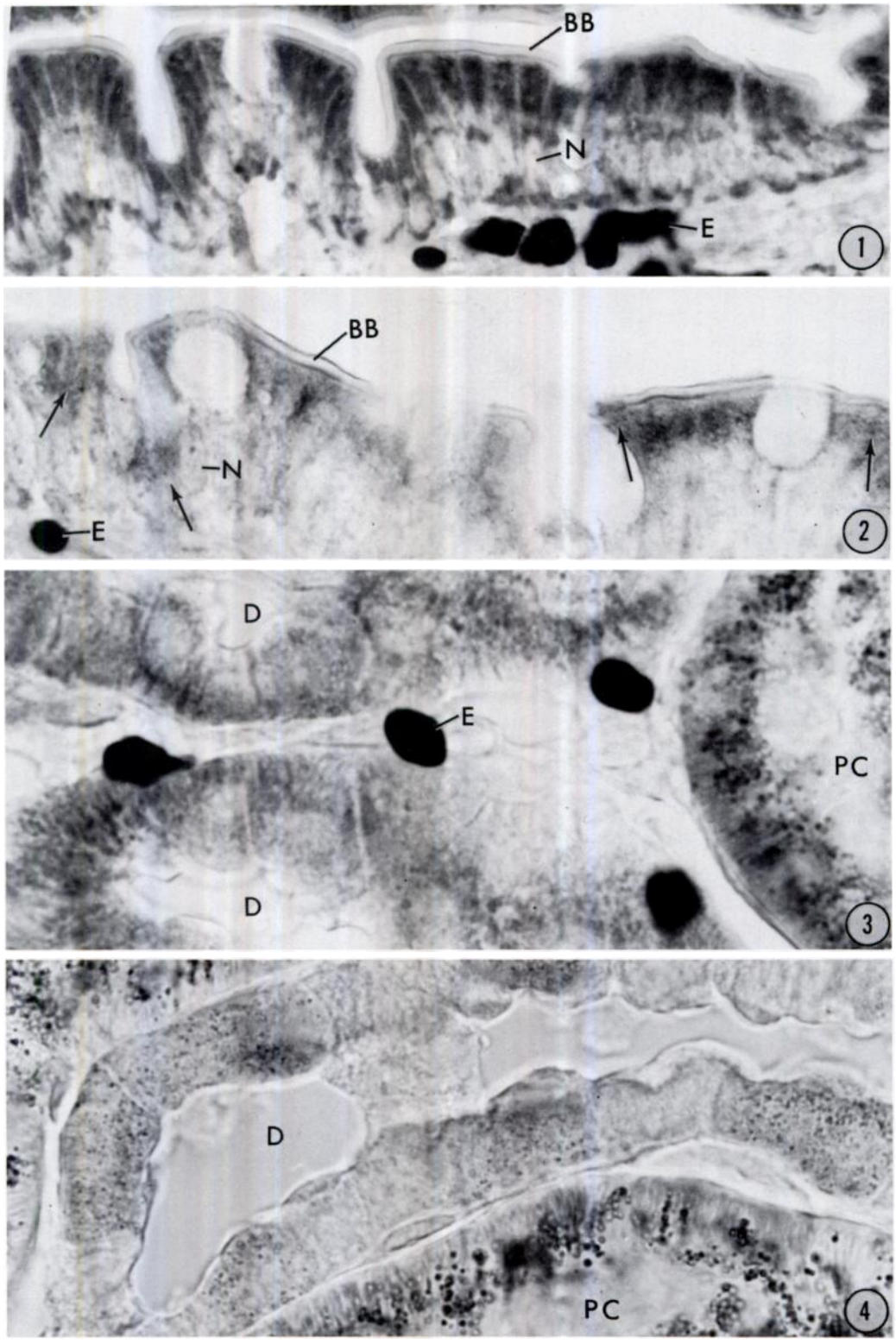
BB
N
E
1
BB
N
E
2
D
E
PC
D
3
D
PC
4

There are some cells that are richer than others in mitochondrial nicotinamide adenine dinucleotide-tetranitro blue tetrazolium reductase activity (45). Similarly, some cells possess larger and apparently more active lysosomes, as judged by both lead and pararosanilin procedures for acid phosphatase and the pararosanilin methods for β-glucuronidase and β-glucosaminidase.[5] It has not yet been determined whether the mitochondria-active cells and the lysosome-active cells are the same and whether they correspond to the DAB-positive cells.

Electron microscopy reveals that the DAB-positive cells are filled with a great many microperoxisomes (Figs. 13 and 17). They range from 0.15 to 0.25 μ in diameter (circular profiles) or in length (elongate profiles), with an average of 0.19 μ. Only two microperoxisomes are outside this range, one 0.30 μ in diameter (circular profile) and one 1.0 μ in length (elongate form) (Fig. 15). Some appear in clusters (Figs. 13 and 14) but the clusters are neither as numerous nor as large as in human jejunum. Numerous continuities between smooth ER and microperoxisome membrane are seen, including multiple continuities to the same microperoxisome (Figs. 14–16 and 19–21). Elongate forms are frequently encountered (Fig. 15). In some cells, the smooth ER is apparently vesiculated and lipid-like droplets are seen within the vesicles (or dilated portions of ER?); often, microperoxisomes are adjacent to these structures (Figs. 21 and 22).

The DAB-negative cells possess structures (Figs. 17–20) of approximately the same size (0.20–0.30 μ in diameter or length), apparent internal structure and continuities with smooth ER (Figs. 18–20) as displayed by the DAB-positive microperoxisomes. Whether these should be considered as microperoxisomes despite their lack of demonstrable catalase is considered in the Discussion.

Thick limbs of Henle in guinea pig: Cells in the thick limb have not been studied extensively by electron microscopy. However, it is evident from light microscopy that this portion of the renal tubule lacks the DAB-positive cells present in the distal tubule and illustrated in Figure 4. Only with great difficulty may an occasional microperoxisome be seen in frozen secions or "thick" Epon sections.

With electron microscopy DAB-positive microperoxisomes are seen but they are few in number, smaller than those in the distal convolution cells and with much less reaction product. Elongate forms are common, with lengths ranging from 0.20 to 0.30 μ and widths from 0.10 to 0.17 μ. Most circular forms vary in diameters from 0.12 to 0.22 μ, and very few are larger, reaching 0.30 μ. As with other microperoxisomes, multiple membrane continuities with smooth ER are evident. Their internal structure is also like that of microperoxisomes in other cells.

DISCUSSION

The pH 9.7 DAB medium: The two cell types studied in this communication illustrate the striking ability of the newly devised alkaline DAB medium to visualize microperoxisomes at the light microscope level; see also Figure 1 in Reference 46. The new medium also yields considerably faster staining of the larger peroxisomes of mammalian hepatocytes and kidney proximal convolution, *i.e.*, it is more "optimal" than previous alkaline DAB media for peroxisomes generally.

[5] The results with naphthol AS-LC N-acetyl-β-D-glucosamine as substrate on glutaraldehyde-fixed kidney are superior to those illustrated by Hayashi (22, 23) with formaldehyde-fixed kidney using the naphthol AS-BI salt. After only 10 min of incubation cells in all portions of the tubule, from glomerulus to collecting ducts, show deeply stained lysosomes of variable size and number.

FIG. 1. Frozen section of human jejunum, fixed in 2.5% glutaraldehyde for 3 hr and incubated for 120 min in the pH 9.0 medium. The cytoplasm between the brush border (BB) and nuclei (N) is darkly stained, largely because of mitochondria. Staining, also due mostly to mitochondria, is present in the infranuclear cytoplasm. Erythrocytes (E) stain intensely. ×750.

FIG. 2. Section prepared as in Figure 1, except that incubation is in the new medium (pH 9.7, with KCN), 120 min. Because mitochondrial staining is inhibited, the dotlike microperoxisomes are evident (arrows). Most are supranuclear but many are present in the infranuclear cytoplasm; some may be seen above the deeply stained erythrocyte (E). ×750.

FIG. 3. Frozen section of guinea pig kidney, fixed in 2.5% glutaraldehyde for 3 hr and incubated for 90 min in the pH 9.0 medium. In the proximal convolution (PC) the peroxisomes are seen against a background of light mitochondrial staining. In the convoluted portion of the distal tubule (D) the background mitochondrial staining obscures the stained microperoxisomes. The intensely stained erythrocytes (E) have been dislodged from the peritubular capillaries. ×1,250.

FIG. 4. Section prepared as in Figure 3, except that incubation is in the new medium, 90 min. Numerous microperoxisomes can now be seen in many cells of the convoluted portion of the distal tubule (D); some cells do not show microperoxisomes. Note that, as previously described (39), peroxisomes of the proximal tubule are seen more clearly. ×1,250.

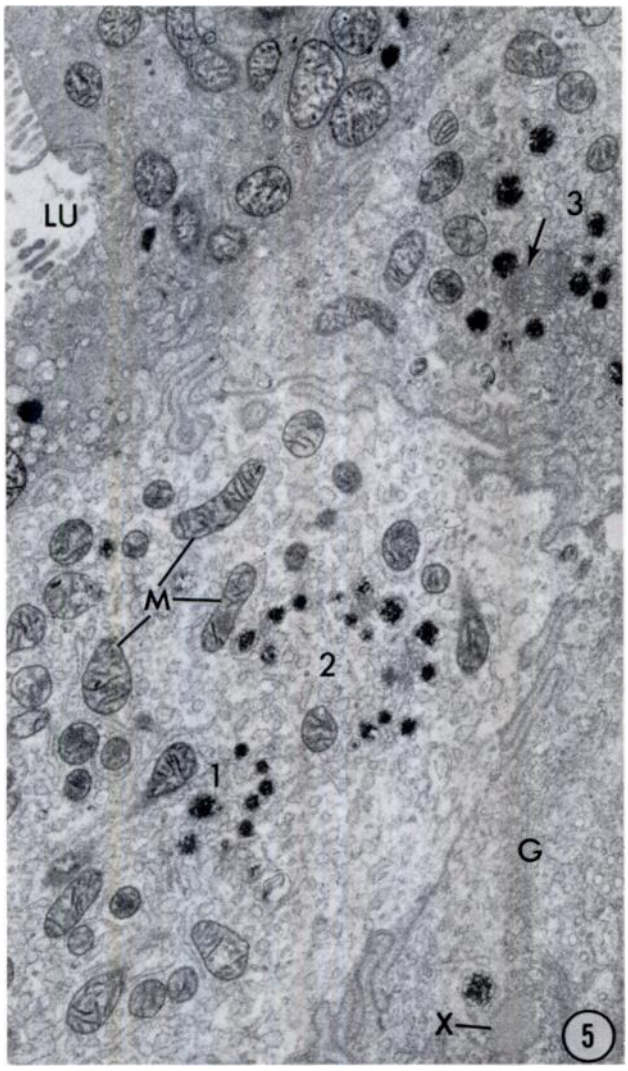
LU
3
M
2
1
G
X
5

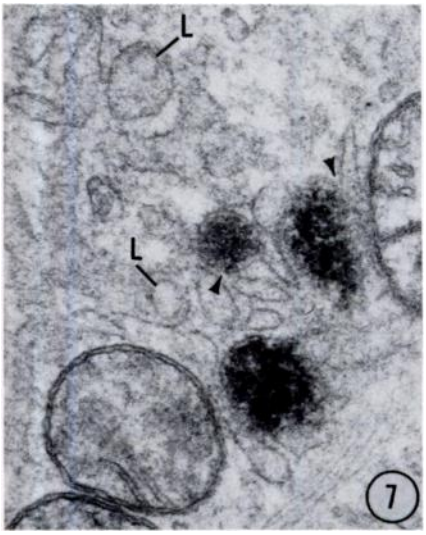
L
L
7

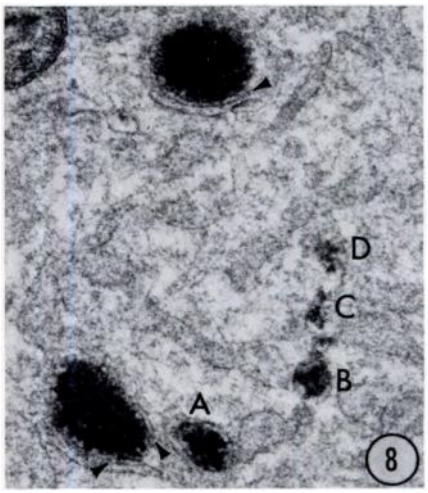
D
C
B
A
8

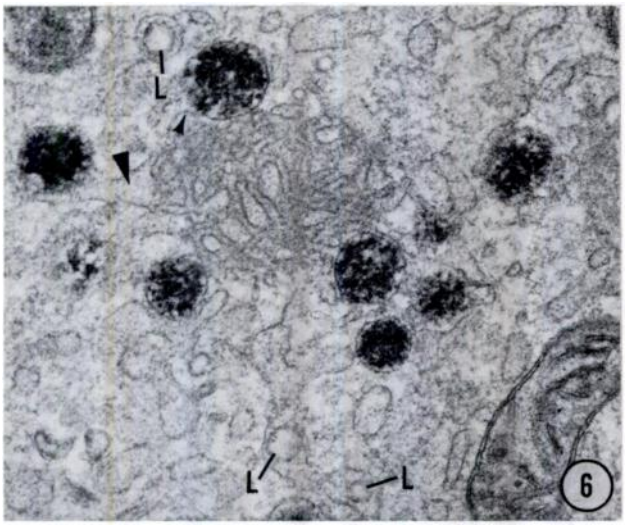
L
L
L
6

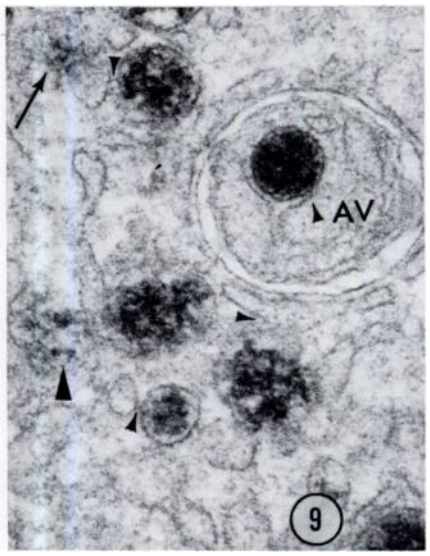
AV
9

The key ingredient for making microperoxisomes visible for light microscopy is potassium cyanide. It is therefore difficult to explain two recent reports that 1×10^{-2} *M* KCN inhibits the peroxisomes (microperoxisomes, by our definition) in cells of rat adrenal cortex (31) and the interstitial cells (Leydig cells) of testes of rat and mouse (52). In the first work from our laboratory (38, 39) we reported that even this high KCN concentration did not inhibit peroxisomes of rat hepatocytes and cells in the proximal convolutions of rat kidney. The same is true of microperoxisomes, as reported earlier and confirmed in the present studies.

Since mitochondrial staining is no hindrance in electron microscopic studies, cyanide addition may be considered optional for such studies. In contrast, the other modifications of the medium are useful for both electron microscopy and light microscopy.

Because of their small size (0.13–0.30 μ) and their clustered distribution in the absorptive cells of human jejunum, it is probable that many of the dots seen in these cells by light microscopy represent overlapping of individual microperoxisomes with reaction product. The same may be true, but to a lesser extent, in the cells of the distal convolutions of the guinea pig kidney. In cells of the thick limbs of Henle the microperoxisomes are few in number and generally not clustered. This probably contributes to our inability to see, by light microscopy, microperoxisomes which are DAB-positive when viewed in the electron microscope. Their degree of staining is not as strong as in other cell types and this, too, helps make these microperoxisomes invisible by light microscopy. The situation is similar in the absorptive cells of rat duodenum. It is possible that further modification of the incubation medium would make such microperoxisomes visible in the light microscope.

Heterogeneity of microperoxisomes: In the DAB-negative cells of the distal tubules in the guinea pig kidney, particles with the fine structure of microperoxisomes are present but they show no reaction product even by electron microscopy. Perhaps their requirements for DAB reactivity are different. This would indicate a heterogeneity among microperoxisomes. Such heterogeneity within the same cell type would be even more striking were

FIGS. 5–12. Portions of absorptive cells in human jejunum, fixed in 2.5% glutaraldehyde for 3 hr and incubated for 90 min at pH 9.7, without KCN. Thin sections are stained with lead citrate (53). The electron density of the microperoxisomes is due to accumulation of reaction product (oxidized DAB).

FIG. 5. Four cells, obliquely sectioned. Only a small portion of the lumen (LU) is included and the basal portions of the cells are not seen. The no. 1–3 indicate three clusters of microperoxisomes. The arrow at 3 indicates a specialized ER domain around which the microperoxisomes are clustered; the area is seen at higher magnification in Figure 6. Barely evident at this low magnification is a portion of the Golgi apparatus (G). A structure marked X is nearby; note the microperoxisome adjacent to it. Such structures are seen at higher magnification in Figures 11 and 12. Some cristae of mitochondria (M) show DAB reaction product. ×10,500.

FIG. 6. Area 3 of the cell in Figure 5, at higher magnification. The specialized ER domain is seen to better advantage. Within the domain the ER is more compact than elsewhere and its cisternae are relatively narrow. The domain has a moderate electron opacity. All but one of the microperoxisomes are connected to the central ER domain, and that one may have been similarly connected outside the plane of section. Lipid-like droplets (L) are seen within the ER, the lower two in a cisterna radiating toward the central ER domain. The small arrowhead indicates a continuity of ER and microperoxisome membrane. The large arrowhead shows a radiating cisterna connected at the left to the microperoxisome and at the right to the central domain. ×37,000.

FIG. 7. Portions of the ER radiating to the microperoxisomes are evident in this field. Note the two lipid droplets (L) within its cisterna. The arrangement of ER and microperoxisomes suggests that they may have been at the edge of a central ER domain. The arrowheads indicate continuities of ER and microperoxisome membrane. ×36,000.

FIG. 8. Four accumulations of reaction product are indicated by A–D. They are connected in a manner suggesting that microperoxisomes are localized swellings of smooth ER. It is possible that in progressing from A to D the microperoxisomes are sectioned more tangentially. Continuities of microperoxisome and smooth ER membrane are indicated by arrowheads. ×48,000.

FIG. 9. This area shows a microperoxisome, still DAB-reactive and maintaining its continuity (arrowhead) with smooth ER, within a structure which is probably an early autophagic vacuole (AV). The arrow indicates a portion of a microperoxisome that may be interpreted as a dilated region of smooth ER; *cf.* Figures 17, 18 and 20 in Reference 46. A similar area may be present at the large arrowhead. Continuities between the membrane of smooth ER and microperoxisomes are indicated by the small arrowheads. ×38,000.

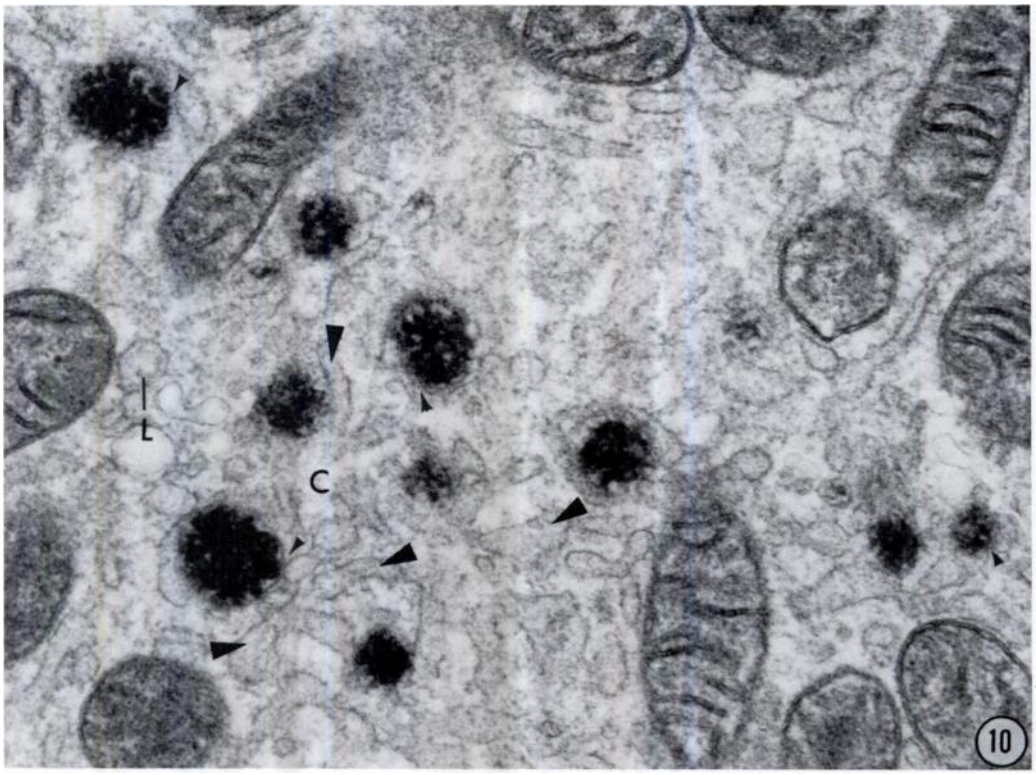
L
C
10

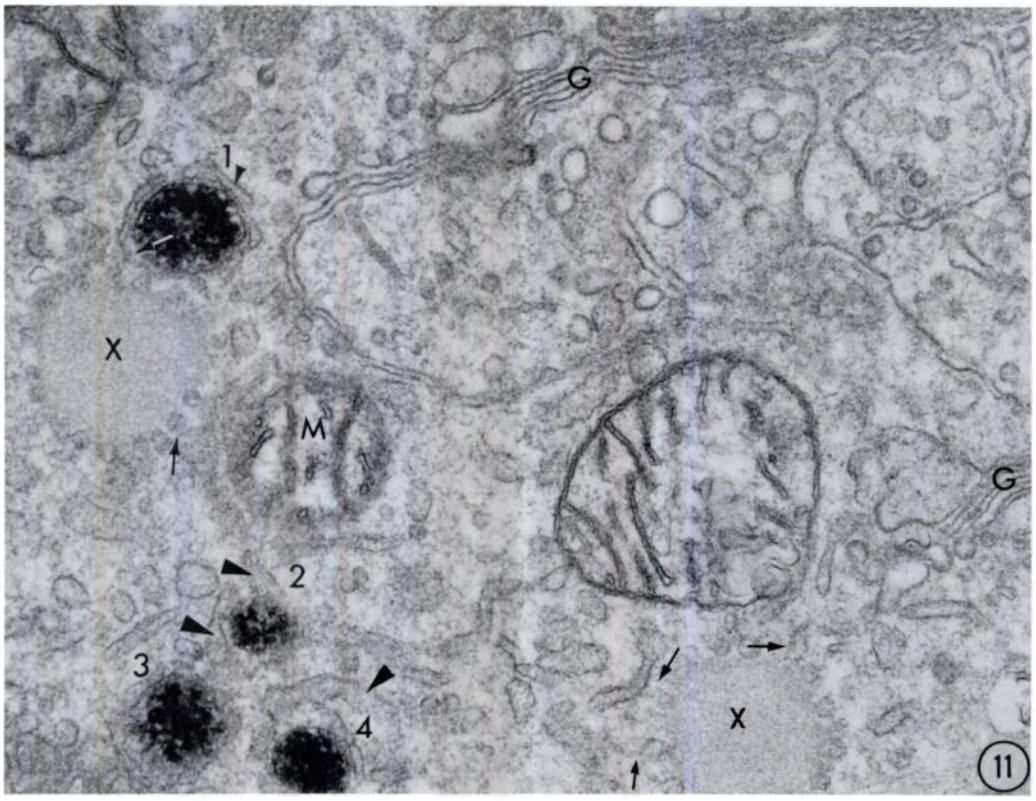
G
1
X
M
G
2
3
4
X
11

catalase indeed absent from these microperoxisomes. This situation would raise anew the question of definition, discussed at length in the first publication in this series (46) in which interesting observations by Graves, Hanzely and Trelease (21) with *Euglena gracilis* suggest the possibility of the absence of catalase activity in particles with H_2O_2-producing oxidase activities. From our vantage point as morphologically oriented cytologists, we would emphasize the common fine structural features of microperoxisomes in a wide variety of cell types: multiple slender continuities with smooth ER, best revealed when the specimen is viewed at different angles (see Figs. 27, 28 and 31-33 in Reference 46); a characteristic internal appearance without a nucleoid or core; and often a tortuous outer membrane. Now that so many cell types have been studied, for us the electron microscopic appearance could outweigh the original biochemical definition of peroxisomes by de Duve and Baudhuin (12, 13), although it is evident that the biochemical definition was essential for the morphologic work and the biochemical base endows meaning to the cytologic observations.

In the two cells described in the present communication, as in about 25 other cell types examined by electron microscopy in our laboratory, the microperoxisomes are continuous with smooth ER. In none of these cells do we find adjacent ribosomes with reaction product, as reported by some investigators (16, 29, 54, 62) and taken by them to mean the synthesis or assembly of catalase on these ribosomes. It has been demonstrated recently (42) that diffusion and adsorption artifacts may occur in DAB cytochemistry. We consider that such artifacts account for the observations of these investigators (42, 46).

Relations of microperoxisomes and lipid: In 1965 Hess, Staubli and Riess (25) administered the hypolipidemic drug, ethyl-α-(*p*-chlorophenoxy) isobutyrate (CPIB), to male rats for 7 days. They observed that the reduced levels of total lipid, phospholipid and cholesterol in the liver were accompanied by the appearance of "microbody-like structures" which "were mostly without cores, indicating that CPIB had caused the formation of an incomplete and aberrant type of organelle." The magnification of the single electron micrograph published was too low to make identification of the organelle as a microperoxisome, but microperoxisomes are present in normal liver (47) and the studies of Reddy and Svoboda on CPIB-treated acatalasemic mice (51) show a marked increase in organelles which we interpret as microperoxisomes. In a more recent study Reddy and Svoboda (52) describe small peroxisomes lacking "the crystalline core or the nucleoid" in the interstitial cells (Leydig cells) of testes of rats and mice. These peroxisomes are surely microperoxisomes, judging from the electron micrograph. Reddy and Svoboda point out that 60% of the rat's cholesterol requirement is synthesized by the testes, and they suggest that a role for these peroxisomes should be considered in the "transport and storage of androgens and cholesterol." Microperoxisomes have been seen in cells of the adrenal cortex in rats and guinea pigs (3, 6, 31); the typical relations to ER have been described by Black[6] (7) in fetal and adult guinea pigs. In our previous publication (46) in which enormous numbers of microperoxisomes were reported in absorptive cells of guinea pig and rat small intestine, we considered it likely that these organelles were related

[6] Black VH: Personal communication.

FIG. 10. Seven microperoxisomes are seen in a cluster (C), surrounded by smooth ER to varying degrees. Membrane continuities of microperoxisomes and smooth ER are indicated by small arrowheads. Note the radiating ER (large arrowheads). L, lipid-like droplets. ×38,500.

FIG. 11. A portion of the Golgi apparatus (G) is included in this field. Near it there are many vesicles or tubules, varying in size and electron opacity. Some resemble the vesicles or tubules which surround the two spherical bodies marked X. There are suggestions (arrows) that short tubules connect the spherical bodies with smooth ER. At the arrow with the white shaft the tubule from the spherical body is seen to be continuous with the smooth ER which surrounds the microperoxisome. Small arrowhead indicates continity of ER and microperoxisome membrane. Note the close proximity of the tangentially sectioned mitochondrion (M) and smooth ER. The latter is continuous with a tubule (arrow) adjacent to the spherical body; it may also be continuous with the ER cisterna radiating to microperoxisome 2 (large arrowhead). Large arrowheads also indicate ER radiating toward microperoxisomes 3 and 4. A small part of the central ER domain is seen at the lower left edge of the figure. ×36,000.

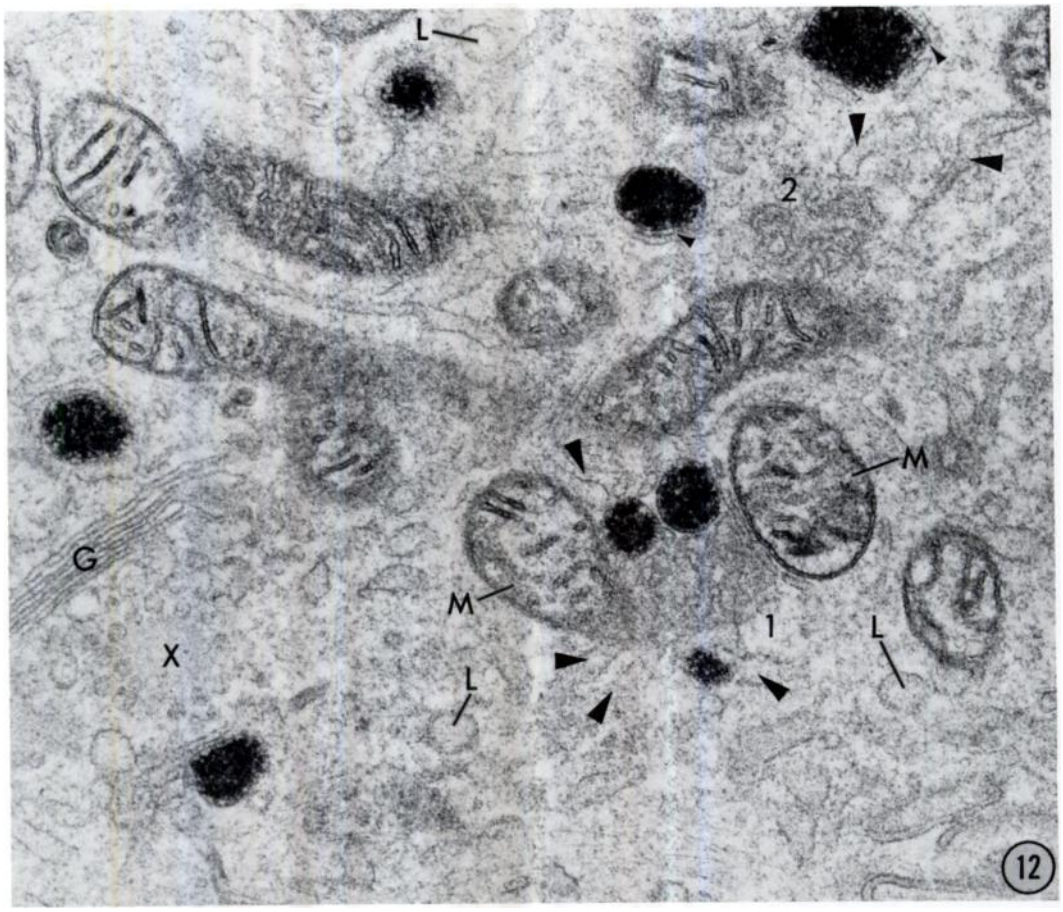

FIG. 12. This field illustrates two central ER domains (1 and 2), microperoxisomes at the periphery of such domains (at 1), radiating ER (large arrowheads) and lipid-like droplets (L) within the ER. Note the proximity of mitochondria (M) to the central domain 1. A spherical body marked X is seen close to the Golgi apparatus (G). The body is surrounded by vesicle-like or tubular structures (*cf.* Fig. 11). The small arrowheads indicate continuities of microperoxisome and ER membrane. ×27,000.

to the major function of these cells, "the absorption of lipid from the intestinal lumen and its transport with modification to form chylomicra."

Our current observations on the absorptive cells of human jejunum provide images highly suggestive of a functional role of microperoxisomes in lipid transport and metabolism. They are strategically situated for such a role. Lipid droplets are present within the smooth ER that radiates to the microperoxisomes and in adjacent ER. None is seen within the central domains with specialized ER. The functional significance of the higher degree of ER order within these domains remains to be determined, as does the close proximity of mitochondria to the domains. Whether the electron opacity within the domains has functional meaning is also unclear. The possibility cannot be excluded that the opacities of ER membrane and cisterna and the enclosed cytosol result from better structural preservation of this more compact ER during tissue preparation.

Marked variation in the ER of different cell types has long been recognized (see, *e.g.*, References 17, 50 and 58). Also well known are ER changes in response to physiologic influences or pathologic states. This has been studied most intensively in hepatocytes (*e.g.*, see References 44 and 57–59); absorptive cells of small

intestine have also been studied (8, 18). It is of great interest that the closest morphologic resemblance to the central ER domains of human jejunum is the ER configuration described by Smuckler *et al.* (57–59) in hepatocytes shortly after administration of carbon tetrachloride and called "tubular aggregates." It may not be coincidence that in Figure 6 of Reference 57 two peroxisomes (or microperoxisomes?) are seen at the periphery of a tubular aggregate.

The jejunum specimen is apparently normal by all histologic, cytochemical and electron microscopic criteria known to us. The effect of the patient's diet during the 4½ days prior to surgery is unknown. Toner, Carr and Wyburn (60) refer to "substantial aggregates" of smooth ER in the apical cytoplasm of an absorptive cell in a presumably normal human small intestine (their Fig. 2.15b).

The microperoxisomes are related spatially, and possibly functionally, to the relatively large lipid-like bodies referred to as X in Figures 5, 11 and 12. Many, perhaps most or even all, of the vesicle-like structures surrounding the bodies are in fact short tubules of smooth ER connected to the bodies (Fig. 11). In Figure 11 an ER tubule is seen connected also to the microperoxisome at the periphery of the body. It is of interest that in the carbon tetrachloride-treated hepatocytes described by Smuckler *et al.* "large lipid droplets" are seen surrounded by collections of smooth ER. Figure 32 in Reference 58 shows three microperoxisomes at the periphery of one such collection.

In some cells of the distal convolutions in guinea pig kidney lipid-like droplets are present in enlarged ER regions (or vesiculated ER?). Microperoxisomes are frequently found nearby.

In a forthcoming publication in this series (43) we describe close spatial relations between microperoxisomes, ER and lipofuscin granules in human hepatocytes. Lipofuscin granules contain highly characteristic lipids.

Differentiation of thick limb of Henle and distal convolution: In his 1969 review Rouiller (55) draws support from the work of Young and Wissig (63) on the rat kidney for considering that, in mammals generally, the thick limb of Henle and the distal convolution are divisions of one portion of the nephron, the distal tubule. Young and Wissig write of the thick limbs that "under examination by light microscopy in this study, this segment of the rat appears morphologically identical with segments of the distal tubule located in the cortex." In the same book, Longley's chapter on histochemical reactions (30) and the electron microscopy chapter by Ericsson and Trump (14) adopt essentially the same view. Much of the evidence rests upon study of the rat kidney. In 1960 Novikoff (33) reported cytochemical studies on the rat kidney. He concluded that, "Except for cells in the macula densa, the distal convolution cells are indistinguishable, by our techniques, from the cells in the thick limb of Henle's loop."

The kidney of the guinea pig is strikingly different from that of the rat in all cytochemical reactions studied earlier (33) as well as in alkaline DAB reaction. In both female and male, the distal convolution, but not the thick limb, has a population of cells with large numbers of microperoxisomes readily visible by light microscopy. In the DAB-negative cells of the distal convolution microperoxisomes are present but unreactive in either the pH 9.0 medium or the more optimal pH 9.7 medium. On the other hand, the microperoxisomes of the cells in the thick limb are DAB-positive, albeit to a lesser degree than in the distal convolution cells. They are, in addition, much less numerous than in the distal convolution cells.

The thick limb cells are readily distinguishable from the cells of the distal convolution in the electron microscope. The most obvious differences are found in the plasma membrane and mitochondria. The thick limb cells have much stouter mitochondria oriented more perpendicularly at the cell base. They are separated from each other by deep *linear* infoldings of the plasma membrane that reach high into cell cytoplasm. In the distal convolution cells the mitochondria, although still large, are considerably shorter and narrower than those of thick limb cells. Not as many are perpendicular to the cell base. The plasma membrane does not have the deep linear infoldings. It is characterized instead by extremely tortuous infoldings near the cell base, roughly *parallel*

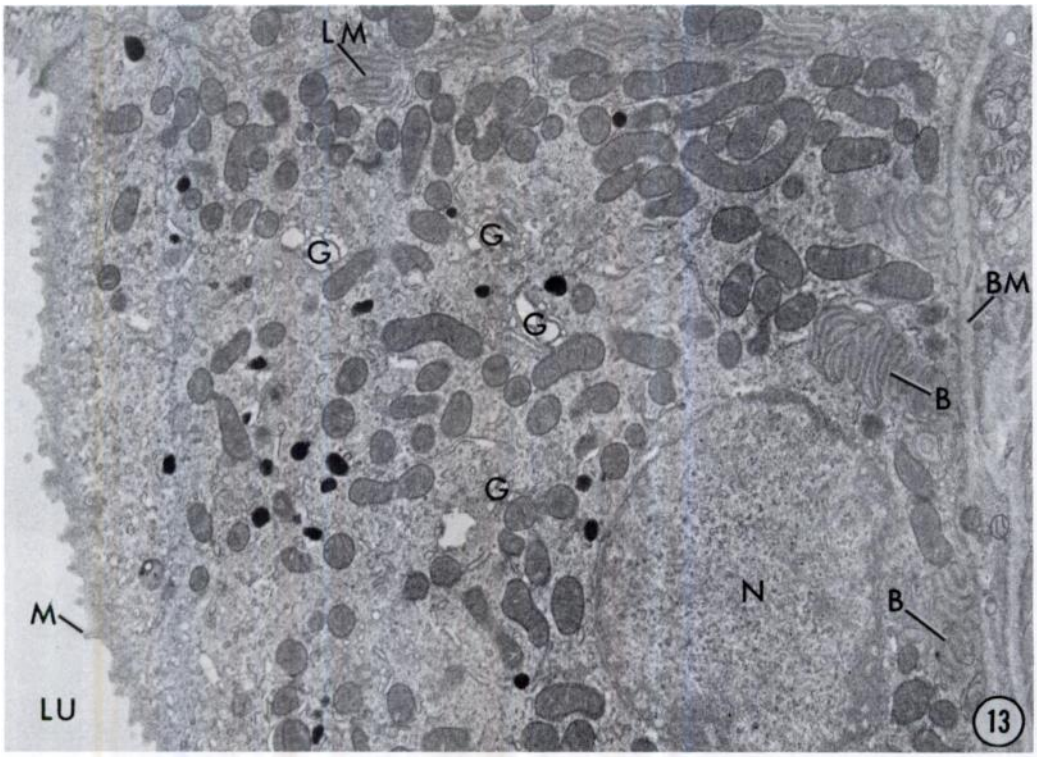
LM
G
G
G
G
BM
B
N
B
M
LU
13

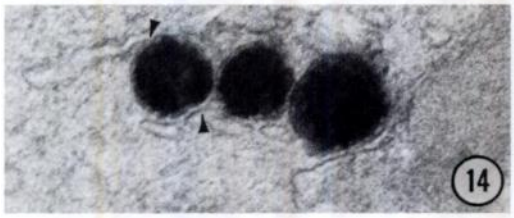
14

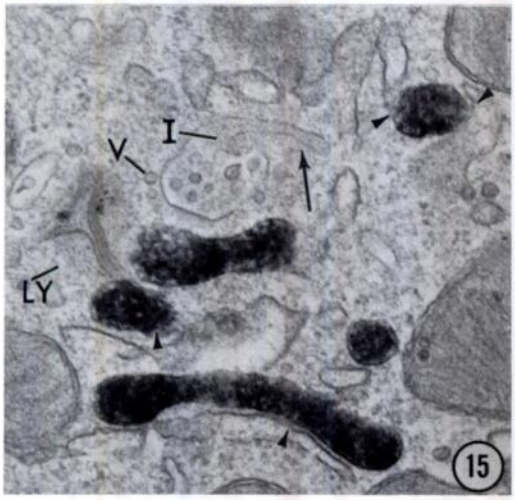
V
I
LY
15

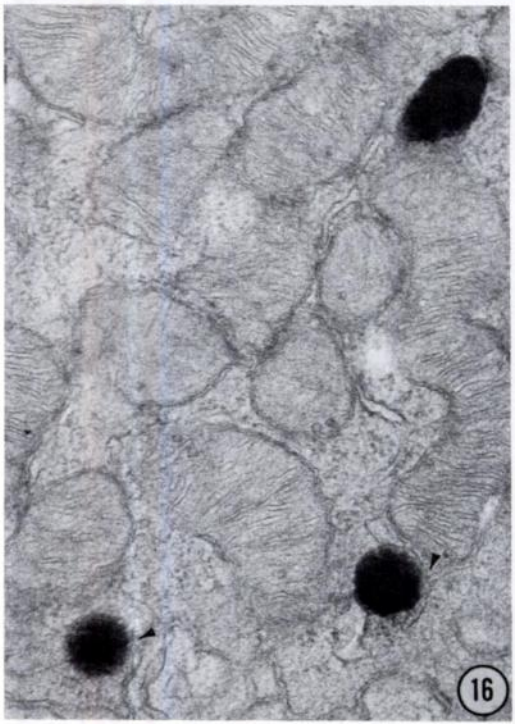
16

FIGS. 13–21. Portions of cells in the convoluted portions of distal tubules of guinea pig kidney, fixed in 2% paraformaldehyde-2.5% glutaraldehyde (32) for 3 hr and incubated for 30 min (Figs. 13 and 15–19) and 60 min (Figs. 12, 14, 20 and 21) at pH 9.7, with KCN. Thin sections are stained with lead citrate (53). The electron opacity of the microperoxisomes is due to accumulation of oxidized DAB.

FIG. 13. Most of the field is occupied by one cell. A small portion of an adjacent cell is seen above the lateral portion of the plasma membrane. Infoldings of this part of the plasma membrane are seen at LM; a junctional complex is seen close to the lumen. The cell occupying most of the field shows short microvilli (M) projecting into the lumen (LU) and infoldings of the plasma membrane (B) adjacent to the basement membrane (BM). Numerous microperoxisomes are seen. Portions of the Golgi apparatus are seen at G; dilations probably represent inadequate preservation. A portion of the nucleus is seen at N. ×9,700.

FIG. 14. Three microperoxisomes, each surrounded by smooth ER. Continuities of ER and microperoxisome membrane are seen at the upper arrowhead and to the right of the lower arrowhead. ×56,000.

FIG. 15. The microperoxisomes in this cluster illustrate: (*a*) the multiple continuities (arrowheads) of ER and microperoxisome membrane and (*b*) the elongate forms commonly seen. A lysosome (LY) is presumably sectioned tangentially so that its delimiting membrane cannot be seen. The arrow indicates a portion of smooth ER interpreted to be continuous with an autophagic vacuole, type II (see Reference 36 and Figs. 30, 34 and 40 in Reference 46), in which ER membrane is thought to internalize, as at I. A vesicle, or transverse section of a tubule, is seen at V; note its resemblance to the structures within the autophagic vacuole. The fuzzy, moderately electron-dense material at the bottom right of the autophagic vacuole is probably a tangentially sectioned membrane where vacuole and ER are in continuity. ×39,000.

FIG. 16. Continuities of smooth ER and microperoxisome membrane are seen at arrowheads. ×36,000.

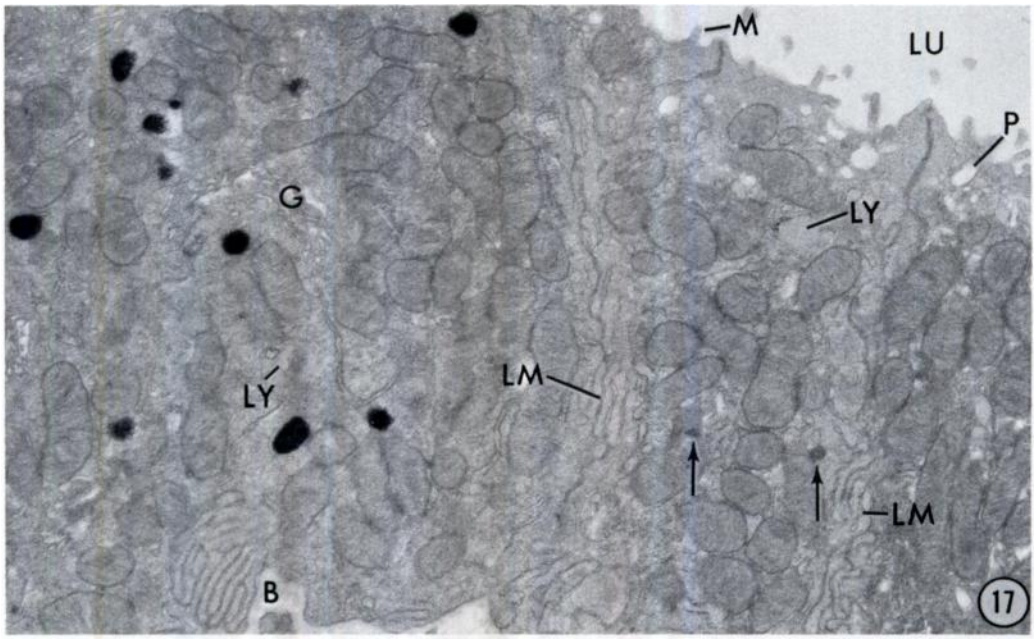
M
LU
P
G
LY
LY
LM
LM
B
17

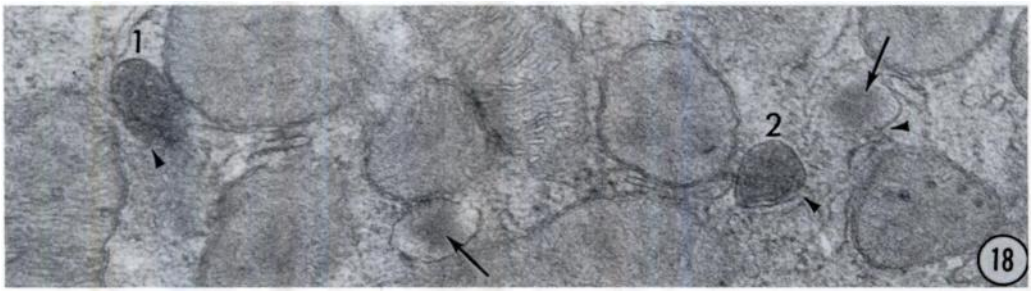
1
2
18

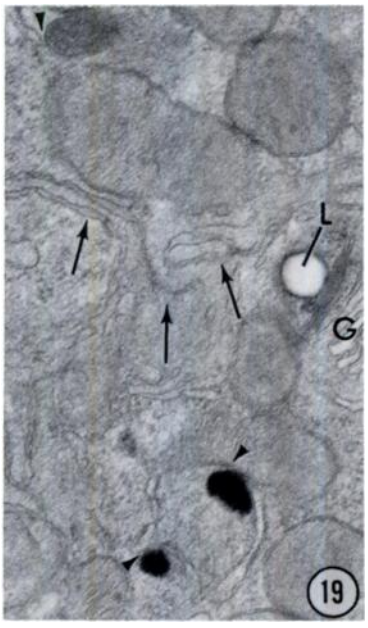
L
G
19


M
P
20

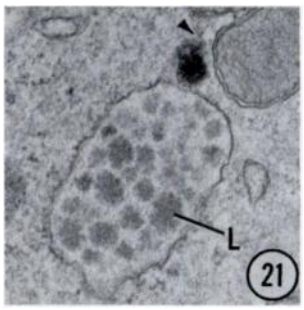
L
21

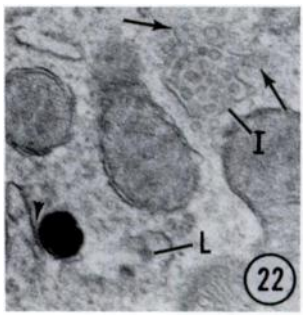
I
L
22

FIG. 17. Portions of three adjacent cells are seen at low magnification. The lateral infoldings (LM) of the plasma membrane indicate the cell limits. Small microvilli (M) project into the lumen (LU). One of the numerous pinocytic vacuoles is seen at P. A part of the basement membrane (B) is evident. A portion of the Golgi apparatus is seen at G. Electron-opaque reaction product is evident in the microperoxisomes of the cell at the left. In the central cell the arrows indicate two microperoxisomes without reaction product. Lysosomes are seen at LY. ×9,500.

FIG. 18. An area of a DAB-negative cell with two microperoxisomes (1 and 2). Both show an internal structure resembling that in DAB-positive microperoxisomes. The arrowheads indicate membrane continuities with smooth ER membrane. It is difficult to identify the two structures to which arrows are directed, one of which shows membrane continuity (arrowhead) with smooth ER. It may be an early form of microperoxisome or, more likely, lipid within the ER cisterna. ×40,000.

FIG. 19. Portions of two adjacent cells. The plasma membrane separating the two cells is indicated by arrows. The bottom cell shows two DAB-positive microperoxisomes. In the cell above, a DAB-negative microperoxisome is seen. All three show continuities of delimiting membranes with smooth ER (arrowheads). L, lipid-like droplets. ×26,000.

FIG. 20. A part of the apical portion of a DAB-negative cell. Some of the numerous pinocytic vesicles are seen (P), as is one of the numerous microvilli (M). Three microperoxisomes without reaction product are seen; arrowheads indicate continuities of microperoxisome membranes with smooth ER membrane. ×36,000.

FIG. 21. A small portion of a cell showing a microperoxisome adjacent to a vacuole that is probably an enlarged region of smooth ER containing lipid-like material (L). The arrowhead indicates a continuity of the microperoxisome membrane with smooth ER. ×28,000.

FIG. 22. This small portion of a cell shows smooth ER continuous with microperoxisome membrane at the arrowhead. Within the ER two lipid-like particles (L) are evident. Also seen is an autophagic vacuole, type II, such as seen in Figure 15. The membranes at the arrows are probably smooth ER; I indicates an area of membrane internalization. ×27,000.

to the underlying plasma membrane, as seen in Figures 13 and 17.

The cells of the two regions differ also in other cytochemical reactions that we have employed. Heterogeneity of reactivity among adjacent cells for mitochondrial nicotinamide adenine dinucleotide-tetranitro blue tetrazolium activity and lysosomal acid phosphatase, N-acetyl-β-glucosaminidase and β-glucuronidase activities is seen in the distal convolution but not in the thick limb.

ACKNOWLEDGMENTS

We are grateful to Mr. Jack Godrich, who prepared the final photographs, and Mrs. Fay Grad for secretarial assistance.

REFERENCES

1. Allen JM, Beard ME: α-Hydroxy acid oxidase: localization in renal microbodies. Science 149: 1507, 1965
2. Barka T, Anderson PJ: Histochemical methods for acid phosphatase using hexazonium pararosanilin as coupler. J Histochem Cytochem 10: 741, 1962
3. Beard ME: Identification of peroxisomes in the rat adrenal cortex. J Histochem Cytochem 20: 173, 1972
4. Beard ME, Novikoff AB: Distribution of peroxisomes (microbodies) in the nephron of the rat: a cytochemical study. J Cell Biol 42:501, 1969
5. Beard ME, Novikoff AB: Reactions of mitochondria with diaminobenzidine. J Cell Biol 43:12, 1969
6. Black VH: Formation of peroxisome-like granules in fetal and adult adrenal cortical cells of guinea pigs. Anat Rec 172:271, 1972
7. Black VH: The development of smooth-surfaced endoplasmic reticulum in adrenal cortical cells of fetal guinea pigs. Am J Anat, in press
8. Cardell RR Jr, Badenhausen S, Porter KR: Intestinal triglyceride absorption in the rat: an electron microscopical study. J Cell Biol 34:123, 1967
9. Chang C-H, Schiller B, Goldfischer S: Small cytoplasmic bodies in the loop of Henle and distal convoluted tubule that resemble peroxisomes. J Histochem Cytochem 19:56, 1971
10. Connock M, Pover W: Catalase particles in the epithelial cells of the guinea-pig small intestine. Histochem J 2:371, 1970
11. Davis BJ, Ornstein L: High resolution enzyme localization with a new diazo reagent, "hexazonium pararosaniline." J Histochem Cytochem 7:297, 1959
12. de Duve C: Evolution of the peroxisome. Ann NY Acad Sci 168:369, 1969
13. de Duve C, Baudhuin P: Peroxisomes (microbodies and related particles). Physiol Rev 46:323, 1966
14. Ericsson JLE, Trump BF: Electron microscopy of the uriniferous tubules, The Kidney, Morphology, Biochemistry, Physiology. Edited by C Rouiller, AF Muller. Vol I. Academic Press, New York, 1969, p 351
15. Fahimi HD: Cytochemical localization of peroxidatic activity of catalase in rat hepatic microbodies (peroxisomes). J Cell Biol 43:275, 1969
16. Fahimi HD: Morphogenesis of peroxisomes in rat liver, Abstracts, American Society for Cell Biology, New Orleans, 1971, p 87
17. Fawcett DW: The Cell, Its Organelles and Inclusions. An Atlas of Fine Structure. WB Saunders Company, Philadelphia, 1966
18. Friedman HI, Cardell RR Jr: Effects of puromycin on the structure of rat intestinal epithelial cells during fat absorption. J Cell Biol 52:15, 1972
19. Goldfischer S, Essner E: Further observations on the peroxidatic activities of microbodies (peroxisomes) J Histochem Cytochem 17:681, 1969
20. Goldfischer S, Essner E: Peroxidase activity in peroxisomes (microbodies) of acatalasemic mice. J Histochem Cytochem 18:482, 1970
21. Graves LB Jr, Hanzely L, Trelease RN: The occurrence and fine structural characterization of microbodies in Euglena gracilis. Protoplasma 72: 141, 1971
22. Hayashi M: Histochemical demonstration of N-acetyl-β-glucosaminidase employing naphthol AS-BI N-acetyl-β-D-glucosaminide as substrate. J Histochem Cytochem 13:35, 1965
23. Hayashi M: Comparative histochemical localization of lysosomal enzymes in rat tissues. J Histochem Cytochem 15:83, 1967
24. Hayashi M, Nakajima Y, Fishman WH: The cytologic demonstration of β-glucuronidase employing naphthol AS-BI glucuronide and hexazonium pararosanilin; a preliminary report. J Histochem Cytochem 12:293, 1964
25. Hess R, Staubli W, Riess W: Nature of the hepatomegalic effect produced by ethyl-chlorophenoxy-isobutyrate in the rat. Nature (Lond) 208:856, 1965
26. Hirai K-I: Light microscopic study of the peroxidatic activity of catalase in formaldehyde-fixed rat liver. J Histochem Cytochem 17:585, 1969
27. Hruban Z, Rechcigl M Jr: Microbodies and related particles. Int Rev Cytol, suppl 1. Academic Press, New York, 1969
28. Kuhn C: Particles resembling microbodies in normal and neoplastic perianal glands of dogs. Z Zellforsch Mikrosk Anat 90:554, 1968
29. Legg PG, Wood RL: New observations on microbodies, a cytochemical study on CPIB-treated rat liver. J Cell Biol 45:118, 1970
30. Longley JB: Histochemistry of the kidney, The Kidney, Morphology, Biochemistry, Physiology. Edited by C Rouiller, AF Muller. Vol I. Academic Press, New York, 1969, p 157
31. Magalhaes MM, Magalhaes MC: Microbodies (peroxisomes) in rat adrenal cortex. J Ultrastruct Res 37:563, 1971
32. Miller F, Herzog V: Die Lokalisation von Peroxidase und sauer Phosphatase in eosinophilen Leukocyten wahrend der Reifung. Elektronenmi-

kroskopisch-cytochemische Untersuchungen am Knochenmark von Ratte und Kaninchen. Z Zellforsch Mikrosk Anat 97:84, 1969
33. Novikoff AB: The rat kidney: cytochemical and electron microscopic studies, Biology of Pyelonephritis. Edited by EL Quinn, EH Kass. Little, Brown and Company, Boston, 1960, p 113
34. Novikoff AB: Cancer cells: enzyme localization and ultrastructure, Proceedings of Symposium of American Cancer Society, October 22-23, 1962. American Cancer Society, New York, 1963, p 60
35. Novikoff AB: Visualization of cell organelles by diaminobenzidine reactions, Seventh International Congress of Electron Microscopy, Grenoble. Edited by P. Favard, Vol 1. Soc Franç Micr Electr, Paris, 1970, p 565
36. Novikoff AB: Lysosomes, a personal account, Lysosomes and Storage Diseases. Edited by G Hers, F Van Hoof. Academic Press, New York, in press
37. Novikoff AB, Beard ME, Albala A, Sheid B, Quintana N, Biempica L: Localization of endogenous peroxidases in animal tissues. J Microsc 12:381, 1971
38. Novikoff AB, Goldfischer S: Visualization of microbodies for light and electron microscopy. J Histochem Cytochem 16:507, 1968
39. Novikoff AB, Goldfischer S: Visualization of peroxisomes (microbodies) and mitochondria with diaminobenzidine. J Histochem Cytochem 17:675, 1969
40. Novikoff AB, Novikoff PM: Cytochemical staining reactions for enzymes in cytoplasmic organelles. Biomembranes 2:33, 1971
41. Novikoff AB, Novikoff PM, Davis C, Quintana N: Studies on microperoxisomes. V. Are microperoxisomes ubiquitous in mammalian cells? Submitted for publication
42. Novikoff AB, Novikoff PM, Quintana N, Davis C: Diffusion artifacts in 3,3'-diaminobenzidine cytochemistry. J Histochem Cytochem 20:745, 1972
43. Novikoff AB, Novikoff PM, Quintana N, Davis C: Studies on microperoxisomes. IV. Relations of microperoxisomes, endoplasmic reticulum and lipofuscin granules. Submitted for publication
44. Novikoff AB, Roheim PS, Quintana N: Changes in rat liver cells induced by orotic acid feeding. Lab Invest 15:27, 1966
45. Novikoff AB, Shin W-Y, Drucker J: Mitochondrial localization of oxidative enzymes: staining results with two tetrazolium salts. J Biophys Biochem Cytol 9:47, 1961
46. Novikoff PM, Novikoff AB: Peroxisomes in absorptive cells of mammalian small intestine. J Cell Biol 53:532, 1972
47. Novikoff PM, Novikoff AB, Quintana N, Davis C: Studies on microperoxisomes. III. Observations on human and rat liver. Submitted for publication
48. Novikoff PM, Novikoff AB, Quintana N, Hauw J-J: Golgi apparatus, GERL, and lysosomes of neurons in rat dorsal root ganglia, studied by thick section and thin section cytochemistry. J Cell Biol 50:859, 1971
49. Petrik P: Fine structural identification of peroxisomes in mouse and rat bronchiolar and alveolar epithelium. J Histochem Cytochem 19:339, 1971
50. Pham TD, Luse SA, Dempsey EW: A unique form of endoplasmic reticulum in endocardial endothelia of the desert iguana. J Ultrastruct Res 39:149, 1972
51. Reddy J, Svoboda D: Microbodies in experimentally altered cells. VIII. Continuities between microbodies and their possible biologic significance. Lab Invest 24:74, 1971
52. Reddy J, Svoboda D: Microbodies (peroxisomes) identification in interstitial cells of the testis. J Histochem Cytochem 20:140, 1972
53. Reynolds ES: The use of lead citrate at high pH as an electron-opaque stain in electron microscopy. J Cell Biol 17:208, 1963
54. Rigatuso JL, Legg PG, Wood RL: Microbody formation in regenerating rat liver. J Histochem Cytochem 18:893, 1970
55. Rouiller C: General anatomy and histology of the kidney, The Kidney, Morphology, Biochemistry, Physiology. Edited by C Rouiller, AF Muller. Vol I. Academic Press, New York, 1969, p 61-156
56. Sabatini D, Bensch K, Barrnett RJ: Cytochemistry and electron microscopy. The preservation of cellular ultrastructure and enzymatic activity by aldehyde fixation. J Cell Biol 17:19, 1963
57. Smuckler EA: Structural and functional alteration of the endoplasmic reticulum during CCl_4 intoxication, Proceedings of the Fourth Meeting of the Federation of European Biochemical Societies, Oslo. Edited by FC Gran. Academic Press, London, 1968, p 13
58. Smuckler EA, Arcasoy M: Structural and functional changes of the endoplasmic reticulum of hepatic parenchymal cells. Int Rev Exp Pathol 7: 305, 1969
59. Smuckler EA, Ross R, Benditt EP: Effects of carbon tetrachloride on guinea pig liver. Exp Mol Pathol 4:328, 1965
60. Toner PG, Carr KE, Wyburn GM: The Digestive System. An Ultrastructural Atlas and Review. Appleton-Century-Crofts, New York, 1971
61. Venkatachalam MA, Soltani MH, Fahimi HD: Fine structural localization of peroxidase in the epithelium of large intestine of rat. J Cell Biol 46:168, 1970
62. Wood RL, Legg PG: Peroxidase activity in rat liver microbodies after aminotriazole inhibition. J Cell Biol 45:576, 1970
63. Young D, Wissig SL: A histologic description of certain epithelial and vascular structures in the kidney of the normal rat. Am J Anat 115:43, 1964